Magnetic Raman Scattering in Two-Dimensional Spin-1/2 Heisenberg Antiferromagnets: Spectral Shape Anomaly and Magnetostrictive Effects

Franco Nori,[1] R. Merlin,[1] Stephan Haas,[2] Anders W. Sandvik,[2] and Elbio Dagotto[2]

[1]*Department of Physics, The University of Michigan, Ann Arbor, Michigan 48109-1120*

[2]*Department of Physics and National High Magnetic Field Laboratory, Florida State University, Tallahassee, Florida 32306*

(Received 23 February 1995)

We calculate the Raman spectrum of the two-dimensional spin-1/2 Heisenberg antiferromagnet by exact diagonalization and quantum Monte Carlo techniques on clusters of up to 144 sites. On a 16-site cluster, we consider the phonon-magnon interaction which leads to random fluctuations of the exchange integral. Results are in good agreement with Raman scattering experiments on various high-T_c precursors, such as La_2CuO_4 and $YBa_2Cu_3O_{6.2}$. In particular, our calculations reproduce the broad line shape of the two-magnon peak, the asymmetry about its maximum, the existence of spectral weight at high energies, and the observation of nominally forbidden A_{1g} scattering.

PACS numbers: 78.30.Hv, 74.72.Jt , 75.50.Ee

Raman scattering is a powerful technique to study electronic excitations in strongly correlated systems. Recently, much attention has been given to the anomalous magnetic scattering with a very broad and asymmetric line shape observed in the Raman spectra of the parent insulating compounds of high-T_c superconductors, such as La_2CuO_4 and $YBa_2Cu_3O_{6.2}$ at around 3230 and 3080 cm^{-1}, respectively [1]. The selection rules associated with this peak are also anomalous. While the spin-pair excitations scatter predominantly in the allowed B_{1g} channel, there is also a significant contribution in the nominally forbidden A_{1g} configuration, as well as much weaker B_{2g} and A_{2g} scattering [1].

Previous theoretical studies on the spin-1/2 Heisenberg model for 2D square lattices have computed the Raman spectra and its moments for a nearest-neighbor interaction [2–5], and *only* the moments when spin interactions along the plaquette *diagonal* were also included [6]. These show good agreement with experiments in regard to the position of the two-magnon peak, but they fail to account for the spectral *shape* and its enhanced *width*.

Several schemes have been considered to resolve this problem. Initially, from the analysis of the moments it was proposed that strong quantum fluctuations were responsible for the broadening (see, e.g., Refs. [2,6]). However, recent studies of spin-pair excitations in a *spin*-1 insulator, $NiPS_3$, show a width comparable to that of the spin-1/2 cuprates [7]. This questions the view that the observed anomaly is due to large quantum fluctuations intrinsic to spin-1/2 systems. We remark that the measured widths are 3–4 times larger [8] than those predicted by Canali and Girvin [5] within spin-wave theory using the Dyson-Maleev transformation, even when processes involving up to four magnons are taken into account. The works by Canali and Girvin [5] and other groups [9,10] present convincing evidence that the observed anomalous features of the magnetic scattering *cannot* be satisfactorily explained by only considering quantum fluctuations.

In order to explain the observed anomalously broad and asymmetric line shapes, it then seems necessary to invoke an additional process. Here, we consider the interaction between magnon pairs and phonons [11]. This mechanism is motivated in part by recent experimental observations of a strong broadening of the B_{1g} and an enhancement of the A_{1g} scattering with increasing temperature [12]. In our approach we consider the phonons as static lattice distortions which induce changes, δJ_{ij}, in the exchange integral J of the undistorted lattice. We calculate the Raman spectra for a *nearest-neighbor* Heisenberg model using a *nearest-neighbor* Raman operator in the quenched-phonon approximation which, like the Born-Oppenheimer approach, focuses on the fast (high-energy) magnon modes and freezes the slow (low-energy) phonons. This approximation is valid for the cuprates because there is a clear separation of energies between the magnetic and vibrational modes. For instance, in $YBa_2Cu_3O_6$ the characteristic Debye frequency is about 340 cm^{-1} while the two-magnon excitation is $\approx$3080 cm^{-1}.

Raman line shape without phonon-magnon coupling.— The isotropic Heisenberg Hamiltonian is given by $H_0 = J\sum_{\langle ij\rangle}\mathbf{S}_i\cdot\mathbf{S}_j$, where the notation is standard, and only nearest-neighbor interaction is assumed. For the cuprates, the exchange integral is $J \simeq 1450$ K $\simeq 0.12$ eV. In our study, we obtained the ground state $|\phi_0\rangle$ of H_0 on finite 2D square clusters with N spins and periodic boundary conditions using a Lanczos ($N = 16, 26$) and quantum Monte Carlo (QMC) ($N = 144$) algorithms. We studied zero and finite temperature spectra associated with the *nearest-neighbor* scattering operator [1–4]

$$R = \sum_{\langle ij\rangle}(\mathbf{E}_{\rm inc}\cdot\hat{\boldsymbol{\sigma}}_{ij})\,(\mathbf{E}_{\rm sc}\cdot\hat{\boldsymbol{\sigma}}_{ij})\mathbf{S}_i\cdot\mathbf{S}_j\,, \qquad (1)$$

where $\mathbf{E}_{\rm inc,sc}$ corresponds to the electric field of the incident and scattered photons, and $\hat{\boldsymbol{\sigma}}_{ij}$ is the unit vector connecting sites i and j. In the cuprates, and for nearest neighbors only, the irreducible representations of R are

0031-9007/95/75(3)/553(4)$06.00

B_{1g}, A_{1g}, and E. We concentrate mainly on the dominant B_{1g} scattering, e.g., $\mathbf{E}_{\rm inc} \propto \hat{x} + \hat{y}$ and $\mathbf{E}_{\rm sc} \propto \hat{x} - \hat{y}$.

The spectrum of the scattering operator can be written as

$$I(\omega) = \sum_n |\langle \phi_n | R | \phi_0 \rangle|^2 \delta[\omega - (E_n - E_0)], \qquad (2)$$

where ϕ_n denotes the eigenvectors of the Heisenberg model with energy E_n. When doing exact diagonalizations on small clusters, the dynamical spectrum $I(\omega)$ is extracted from a continued fraction expansion of the quantity

$$I(\omega) = -\frac{1}{\pi} \mathrm{Im} \langle \phi_0 | R \frac{1}{\omega + E_0 + i\epsilon - H_0} R | \phi_0 \rangle, \qquad (3)$$

where ϵ is a small real number introduced in the calculation to shift the poles of Eq. (3) into the complex plane. In the QMC simulations, the imaginary-time correlator $\langle R(\tau) R(0) \rangle$ is calculated and $I(\omega)$ is obtained by numerically continuing this function to real frequencies using a maximum entropy procedure [13].

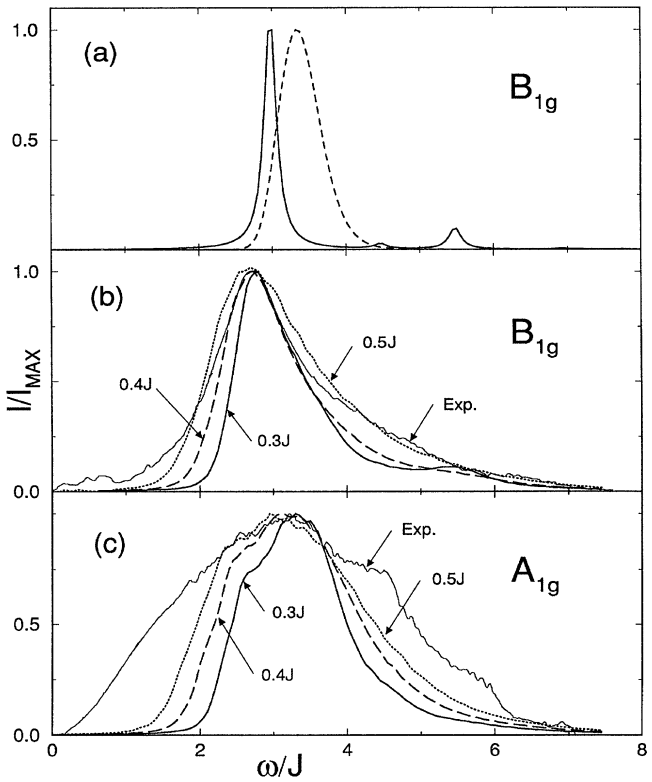

FIG. 1. Normalized Raman cross section, $I(\omega)/I_{\rm max}$, versus ω/J, for the spin-1/2 Heisenberg model with N sites. (a) B_{1g} Raman spectra obtained from exact diagonalization with $N = 16$, $T = 0$, and $\epsilon = 0.1J$; and from QMC with $N = 144$ and $T = J/4$. B_{1g} (b) and A_{1g} (c) spectra obtained from exact diagonalization ($N = 16$) with randomness in the exchange integral representing the interaction between spin-pairs and the phonons. The continuous, dashed, and dotted lines in (b) and (c) correspond, respectively, to $\sigma = 0.3J$, $0.4J$, and $0.5J$. For comparison, the experimental results (from Ref. [6]) are shown.

Our calculated B_{1g} spectra, not including phonon effects, are shown in Fig. 1(a). They were obtained from exact diagonalization ($N = 16$) and QMC ($N = 144$) studies of the Heisenberg Hamiltonian on square lattices. The two-magnon excitation observed experimentally lies around $3J$, which is in good agreement with the location of the main peak obtained from exact diagonalization in Fig. 1. The position of this peak can be understood in terms of the Ising model, which corresponds to the limit of the anisotropic Heisenberg Hamiltonian when no quantum fluctuations are present. In its ground state, the Ising spins align antiferromagnetically for $J > 0$. Within this model and for a 2D square lattice, the incoming light creates a local spin-pair flip at an energy $3J$ higher than the ground state energy. This argument remains approximately valid even in the presence of quantum fluctuations [2–5]. Our results indicate that the two-magnon excitation is at $2.9757J$, $3.0370J$, and $3.2J$ for the 16-, 26-, and 144-site square lattices, respectively. Finite-size effects are small because of the local nature of the Raman operator. For the 144-site lattice, the QMC calculation was carried out at a temperature $T = J/4$. The slight shift of the peak position, compared to the $T = 0$ results for the smaller clusters, is consistent with the finite-T exact diagonalization results of Ref. [3]. Statistical errors, absent in the exact diagonalization results but unavoidable in any stochastic simulation, enhance the width of the 144-site spectrum. These results confirm that neither finite-size effects nor finite temperature can account for the discrepancies with the experimental spectra. The fact that the calculated width is considerably smaller than the experimental one indicates that magnetic quantum fluctuations alone are not the source of the width anomaly.

Line-shape anomaly.—The Raman spectra obtained from the pure Heisenberg model [see Fig. 1(a)] show good agreement with experiments in regard to the two-magnon peak position, but the calculated width is too small. We will consider here the coupling between the magnon pair and phonons [11,12] to account for the observed wide and asymmetric line shape. Our mechanism relates to that proposed by Halley [14] to account for two-magnon infrared absorption in, e.g., MnF_2.

Quantum and thermal fluctuations distort the lattice. The exchange coupling, which depends on the instantaneous positions of the ions, can be expanded in terms of their displacements from equilibrium $\mathbf{u}$. Keeping only the dominant linear terms: $J_{ij}(\mathbf{r}) = J_{ij} = J + \delta J_{ij} = J + \mathbf{u} \cdot \nabla J_{ij}(\mathbf{R})$. Here, δJ_{ij} represents the instantaneous value of $\mathbf{u} \cdot \nabla J_{ij}(\mathbf{R})$, where $\mathbf{R}$ denotes the equilibrium position of the ion carrying the spin (located at $\mathbf{r} = \mathbf{R} + \mathbf{u}$). In the quenched-disorder approximation, the effective Hamiltonian is

$$H_1 = \sum_{\langle ij \rangle} (J + \delta J_{ij}) \mathbf{S}_i \cdot \mathbf{S}_j, \qquad (4)$$

where $|\delta J_{ij}| < J$ is a random variable corresponding to

taking a snapshot of the lattice. This new Hamiltonian is no longer translationally invariant.

In our study, the random couplings δJ_{ij} were drawn from a Gaussian distribution $P(\delta J_{ij}) = \exp[-(\delta J_{ij})^2/2\sigma]/\sqrt{2\pi\sigma}$. $I(\omega)$ was obtained as the quenched average over $m \simeq 1000$ realizations of the randomly distorted lattice. The quenched average of an operator $\hat{O}$ is defined by $\langle\langle \hat{O} \rangle\rangle = (1/m)\sum_{j=1}^{m}\langle \phi_0(j)|\hat{O}|\phi_0(j)\rangle$, where $\phi_0(j)$ is the ground state of the jth realization of the disordered system.

In Fig. 1(b) we show the B_{1g} Raman spectrum from Eq. (1) for a 16-site square lattice in the presence of random exchange couplings with $\sigma \sim 0.4J$, which we found to agree best with experimental spectra at low temperatures [1]. Our calculations do not consider the effect of frozen phonons on the scattering operator R. Notice that the coefficients pertaining to R are generally unrelated to the matrix elements of the system's Hamiltonian (e.g., $\partial J/\partial Q$ in H bears on e^2/r, while the corresponding terms $\propto QS_iS_j$ in R bear on the dipole moment). In particular, and unlike the case without phonons, the fully symmetric A_{1g} component of the scattering operator does not commute with H.

We find that the *three* main features observed in the B_{1g} configuration [1], namely, the broad line shape of the two-magnon peak, the asymmetry about its maximum, and the existence of spectral weight up to $\omega \sim 7J$ are well reproduced. Beyond the two-magnon peak, there is a continuum of phonon-multimagnon excitations. The small feature around $\omega \simeq 5.5J$ (for $0 \leq \sigma \leq 0.3J$) is compatible with a four-magnon excitation.

Magnetostriction.—Since the effects of the phonon-magnon interaction (i.e., magnetostriction) have not been extensively studied by theoretical work in the cuprates, a few comments are in order. The coupling between the spin and strain degrees of freedom modifies both elastic and magnetic properties. In fact, there are extensive studies on the (sometimes very strong) influence of elasticity on magnetism [15–17]. Mattis and Shultz [15] considered the influence of *uniform compression* (i.e., all bonds *equally distorted*) in their classic study of magnetothermomechanics. Their results were criticized [16] for ignoring the effects of phonons (i.e., *local fluctuations* in the bond lengths, which are taken into account in the present work). Recently, *giant* magnetostrictive effects have been reported in several high-T_c superconductors [18]. Also, important magnetostrictive effects have been reported in heavy-fermion [19] and low-T_c [20] superconductors.

Superexchange-phonon coupling.—The width of the Gaussian distribution, σ, represents changes in J due to large *incoherent* atomic displacements. Thus, one can write $\sigma \sim |\langle \delta \ln J/\delta Q\rangle\langle Q\rangle|$ where $\langle Q\rangle$ is an average *zero point motion* (at $T = 0$) and $\langle \delta J/\delta Q\rangle$ is a weighted average of ∇J_{ij} with respect to the displacement of *all* the ions participating in the exchange. Parenthetically, it is trivial to treat the case $T \neq 0$ by increasing δJ. Let r be the Cu-Cu distance, v the sound velocity, and M an effective reduced mass for the ions. A simple calculation gives $\langle Q\rangle/r \sim (Mvr/\hbar)^{-1/2} \sim 0.05$ which is consistent with x-ray measurements of the mean displacement of oxygen atoms normal to the layers [21,22]. While ∇J_{ij} is not known for most phonons, values for longitudinal acoustic modes can be gained from the r dependence of J in the form $J(r) \sim r^{-\alpha}$ or $\partial \ln J/\partial \ln r = -\alpha$ [23]. For conventional transition metal oxides and halides, $10 \leq \alpha \leq 14$ [23], in reasonable agreement with the theoretical estimate $\alpha = 14$ [24]. For the cuprates, high-pressure Raman measurements [25] and material trends [26] give, respectively, $\alpha \approx 5-7$ and $\alpha \approx 2-6$. These values, bearing on the coupling of magnons with *acoustic* phonons translate into $\sigma \approx (0.1 - 0.35)J$. We emphasize that the relevant *incoherent* δJ's (or δQ's) of our case are much larger than those in pressure studies involving *coherent* motion of ions (see, e.g., the discussion on p. 466 of [14]), and that both acoustic and *optical* modes contribute to σ. Thus, we must use larger σ ($\sigma \sim 0.4J$).

Finally, we would like to stress that not every kind of disorder gives rise to the observed broadening of the spectrum. For instance, disorder by point defects or twinning planes will not produce such an effect. Also, it is observed in experiments that the Raman linewidth broadens with increasing temperature [12]. This is a strong indication of a phonon mechanism for the broadening.

A_{1g} and B_{2g} symmetries.—For the A_{1g} symmetry, the undistorted Raman operator commutes with the Heisenberg Hamiltonian, and *no* scattering can take place. However, the addition of disorder changes the commutator and can produce an A_{1g} signal. Nevertheless, the silent B_{2g} channel remains forbidden within our *nearest-neighbor* Raman operator. Figure 1(c) shows the comparison between our numerically obtained A_{1g} spectra (for $\sigma \sim 0.4J$) and the experimental results [1,6]. The slight asymmetry of the A_{1g} line shape is due to four-magnon excitations. The agreement between theory and experiments is reasonably good. However, for $\sigma = 0.3J$, the experimental A_{1g} width is about a factor of 2 broader than the theoretical calculation. We stress that the A_{1g} scattering follows naturally from our model unlike approaches relying on additional hypotheses, like, for instance, diagonal-nearest-neighbor couplings [6], 4-spin terms [9], new fermionic quasiparticles [27], or spinons. For a detailed discussion of these and other proposed explanations of the line shape anomaly, see [5,10].

Extensions.—The midinfrared optical absorption in undoped lamellar copper oxides shows broad features which are believed to originate from exciton-magnon absorption processes [28]. Instead, these results could be interpreted as due to the interaction between phonons and magnons [29]. Also, the inclusion of phonon-induced strong disorder has shown excellent agreement with conductivity experiments [30].

In summary, we find that light scattering spectra by spin excitations is caused by intrinsic spin-spin interactions and by interactions with phonons. We provide strong evidence

that the two-magnon Raman peak is strongly modified by coupling to low-energy phonons which randomly distort the lattice. Our calculations are in good agreement with experiments and provide a simple explanation of four puzzling features of the data: the broad line shape of the two magnon peak, the asymmetry about its maximum, the existence of a spectral weight at high energies, and the observation of nominally forbidden A_{1g} scattering.

We thank J. Riera for his help. S. H. acknowledges support by the Supercomputer Computations Research Institute (SCRI). The work of E. D. and R. M. is partially supported by the donors of The Petroleum Research Fund, and the work of E. D. and A. S. by the ONR Grant No. N00014-93-1-0495.

[1] K. B. Lyons *et al.*, Phys. Rev. B **39**, 2293 (1989); I. Ohana *et al., ibid.* **39**, 2293 (1989); P. E. Sulewski *et al., ibid.* **41**, 225 (1990); T. Tokura *et al., ibid.* **41**, 11 657 (1990); S. Sugai *et al., ibid.* **42**, 1045 (1990).

[2] E. Dagotto and D. Poilblanc, Phys. Rev. B **42**, 7940 (1990).

[3] F. Nori, E. Gagliano, and S. Bacci, Phys. Rev. Lett. **68**, 240 (1992); S. Bacci and E. Gagliano, Phys. Rev. B **43**, 6224 (1991); **42**, 8773 (1990).

[4] Z. Liu and E. Manousakis, Phys. Rev. B **43**, 13 246 (1991).

[5] C. M. Canali and S. M. Girvin, Phys. Rev. B **45**, 7127 (1992).

[6] R. R. P. Singh *et al.*, Phys. Rev. Lett. **62**, 2736 (1989).

[7] S. Rosenblum, A. H. Francis, and R. Merlin, Phys. Rev. B **49**, 4352 (1994).

[8] W. H. Weber and G. W. Ford, Phys. Rev. B **40**, 6890 (1989).

[9] S. Sugai, Solid State Commun. **75**, 795 (1990); M. Roger and J. M. Delrieu, Synth. Met. **29**, F673 (1989).

[10] L. Marville, Ph.D. thesis, Massachusetts Institute of Technology, 1992.

[11] M. J. Massey, R. Merlin, and S. M. Girvin, Phys. Rev. Lett. **69**, 2299 (1992); J. B. Sokoloff, J. Phys. C **5**, 2482 (1972); M. G. Cottam, J. Phys. C **7**, 2901 (1974).

[12] P. Knoll *et al.*, Phys. Rev. B **42**, 4842 (1990).

[13] J. E. Gubernatis *et al.*, Phys. Rev. B **44**, 6011 (1991).

[14] J. W. Halley, Phys. Rev. **154**, 458 (1967).

[15] D. C. Mattis and T. D. Shultz, Phys. Rev. **129**, 175 (1963).

[16] M. E. Fisher, Phys. Rev. **176**, 257 (1968); G. A. Baker and J. W. Essam, Phys. Rev. Lett. **24**, 447 (1970); H. Wagner and J. Swift, Z. Phys. **239**, 182 (1970); H. C. Bolton and B. S. Lee, J. Phys. C **3**, 1433 (1970); F. J. Wegner, *ibid.* **7**, 2109 (1974); E. Pytte, Phys. Rev. B **10**, 2039 (1974); D. J. Bergman and B. I. Halperin, Phys. Rev. B **13**, 2145 (1976); Z.-Y. Chen and M. Kardar, *ibid.* **30**, 4113 (1984).

[17] M. Hase *et al.*, Phys. Rev. Lett. **70**, 3651 (1993); J. P. Pouget *et al., ibid.* **72**, 4037 (1994); K. Hirota *et al., ibid.* **73**, 736 (1994); Q. J. Harris *et al.*, Phys. Rev. B **50**, 12 606 (1994).

[18] H. Ikuta *et al.*, Phys. Rev. Lett. **70**, 2166 (1993); A. del Moral *et al.*, Physica (Amsterdam) **161C**, 48 (1989); A. M. Kadomtseva *et al., ibid.* **162C**, 1361 (1989).

[19] F. E. Kayzel *et al.*, Physica (Amsterdam) **147B**, 231 (1987); A. de Visser *et al., ibid.* **165–166B**, 375 (1990).

[20] M. Isino *et al.*, Phys. Rev. B **38**, 4457 (1988).

[21] G. H. Kwei, A. C. Lawson, and M. Mostoller, Physica (Amsterdam) **175C**, 135 (1991).

[22] A. S. Borovik, A. A. Epiphanov, V. S. Malyshevsky, and V. I. Makarov, Phys. Lett. A **161**, 523 (1992).

[23] See, e.g., M. J. Massey *et al.*, Phys. Rev. B **41**, 8776 (1990), and references therein.

[24] W. A. Harrison, *Electronic Structure and the Properties of Solids* (Freeman, San Francisco, 1980).

[25] M. Aronson *et al.*, Phys. Rev. B **44**, 4657 (1991).

[26] S. L. Cooper *et al.*, Phys. Rev. B **42**, 10 785 (1990).

[27] T. Hsu, Phys. Rev. B **41**, 11 379 (1990); this Raman line shape does not agree with experiments, e.g., the A_{1g} and B_{1g} spectra look almost identical, and the asymmetry has the wrong sign.

[28] J. D. Perkins *et al.*, Phys. Rev. Lett. **71**, 1621 (1993).

[29] R. Merlin *et al.* (unpublished); J. Lorenzana and G. A. Sawatzky (unpublished); J. R. McBride, L. R. Miller, and W. H. Weber, Phys. Rev. B **49**, 12 224 (1994); B. Normand, H. Kohno, and H. Fukuyama (unpublished).

[30] R. Fehrenbacher, Phys. Rev. B **49**, 12 230 (1994).